Acta Crystallographica Section F
Structural Biology and Crystallization Communications
ISSN 1744-3091

Crystallization and preliminary X-ray diffraction analysis of a specific VHH domain against mouse prion protein

Romany N. N. Abskharon,[a,b] Sameh H. Soror,[a,b]* Els Pardon,[a,b] Hassan El Hassan,[a,b] Giuseppe Legname,[c] Jan Steyaert[a,b]* and Alexandre Wohlkonig[a,b]

[a]Structural Biology Brussels, Free University of Brussels, Pleinlaan 2, Brussels 1050, Belgium, [b]Molecular and Cellular Interactions, VIB, Pleinlaan 2, Brussels 1050, Belgium, and [c]International School for Advanced Studies, Institute for Neurodegenerative Diseases, Trieste, Italy

Correspondence e-mail: ssoror@vub.ac.be, jan.steyaert@vub.ac.be

Received 9 July 2010
Accepted 17 October 2010

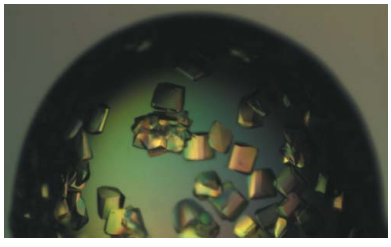

Prion disorders are infectious diseases that are characterized by the conversion of the cellular prion protein PrP^{C} into the pathogenic isoform PrP^{Sc}. Specific antibodies that interact with the cellular prion protein have been shown to inhibit this transition. Recombinant VHHs (variable domain of dromedary heavy-chain antibodies) or nanobodies are single-domain antibodies, making them the smallest antigen-binding fragments. A specific nanobody (Nb_PrP_01) was raised against mouse PrP^{C}. A crystallization condition for this recombinant nanobody was identified using high-throughput screening. The crystals were optimized using streak-seeding and the hanging-drop method. The crystals belonged to the orthorhombic space group $P2_12_12_1$, with unit-cell parameters a = 30.04, b = 37.15, c = 83.00 Å, and diffracted to 1.23 Å resolution using synchrotron radiation. The crystal structure of this specific nanobody against PrP^{C} together with the known PrP^{C} structure may help in understanding the PrP^{C}/PrP^{Sc} transition mechanism.

1. Introduction

Transmissible spongiform encephalopathies (TSEs) or prion diseases are a class of fatal mammalian transmissible neurodegenerative diseases. Notable examples of TSEs include bovine spongiform encephalopathy (BSE), commonly known as mad cow disease; in humans, it is known as new variant Creutzfeldt–Jakob disease (CJD). These disorders are associated with the conversion of the normal cellular prion protein PrP^{C} to its pathogenic isoform PrP^{Sc} (Watts *et al.*, 2009). Prion diseases are characterized by long incubation periods, spongiform changes and the accumulation of misfolded protein deposits. TSEs can arise sporadically, can be inherited or can be transmitted by the infectious form of the prion PrP^{Sc} (McKintosh *et al.*, 2003). The critical event in disease transmission is believed to be the conversion of a monomeric protease-sensitive cellular prion protein, PrP^{C}, into a protease-resistant oligomeric form, PrP^{Sc} (Birkmann & Riesner, 2008).

Previous research has indicated that the transition of PrP^{C} into PrP^{Sc} can be inhibited by antibodies *in vitro* and *in vivo* (Antonyuk *et al.*, 2009). Hence, finding specific PrP^{C} antibodies which can inhibit the transition could help in understanding the pathogenic transition from PrP^{C} to PrP^{Sc}.

Camelidae antibodies are a class of immunoglobulins that lack light chains; they are named heavy-chain antibodies and are also referred to as nanobodies (Nbs; Van den Abbeele *et al.*, 2010). Nbs, which are composed of a single domain, are thus some of the smallest antigen-binding fragments and possess all of the features of conventional antibodies (Lam *et al.*, 2009). However, previous biophysical studies have revealed that camel antibodies possess a number of unique features that are not exhibited by conventional antibodies. A particular advantage is their small size (15 kDa), high solubility and stability (Saerens *et al.*, 2005). Nbs have three hypervariable regions named complementarity-determining regions (CDRs) which may interact with the antigen in concert or independently.

All of these features make Nbs interesting for a broad range of applications such as enzyme inhibition and as diagnostic and ther-

apeutic agents (Smolarek *et al.*, 2010) and more recently as crystallization chaperones (Korotkov *et al.*, 2009; Lam *et al.*, 2009).

To date, several structures of nanobody–protein complexes have been deposited in the PDB; however, only a few structures of a nanobody alone are found. This might be a consequence of the high flexibility of nanobody CDRs, which renders the crystallization of the nanobody alone a difficult process. Homologues of our Nb_PrP_01, with identities in the range 60–70%, are present in the PDB; however, none of them have shown the exceptional high resolution that we have obtained.

Here, we report the crystallization of a specific nanobody (Nb_PrP_01) raised against mouse PrP^{C} ($moPrP^{C}$) in llama.

2. Experimental procedure and results

2.1. Nanobody production, expression and purification

A llama (*Lama glama*) was injected subcutaneously with recombinant $moPrP^{C}$ (23–230). Selection and extraction of the nanobody (Nb_PrP_01) was performed as described previously (Conrath *et al.*, 2001).

The nanobodies of interest were cloned into an *Escherichia coli* expression vector (pHEN6) with a His tag at the C-terminal end. The pHEN6 vector carries a pelB signal peptide for recombinant expression in the periplasm (Conrath *et al.*, 2001). The plasmid was then transformed into *E. coli* WK6 expression strain. A freshly transformed colony was grown overnight in LB medium containing ampicillin (100 µg ml^{-1}) and 1% glucose to make the preculture. The following day, 10 ml preculture was added to 1 l TB medium (supplemented with 100 µg ml^{-1} ampicillin, 2 m*M* $MgCl_2$ and 0.1% glucose) and grown at 310 K until an OD_{600} of 0.7 was reached. Recombinant nanobody expression was induced by addition of IPTG (1 m*M*) and incubation overnight at 301 K.

Recombinant His-tagged nanobody was purified from *E. coli* WK6 cells after periplasmic extraction (Lauwereys *et al.*, 1998) by adding Ni–NTA chelating beads (Qiagen) to the lysate (the lysis buffer was 0.2 *M* Tris pH 8.0, 0.5 m*M* EDTA, 0.5 *M* sucrose). The beads were poured into an empty column (PD10) and washed extensively with washing buffer: 50 m*M* Na_2HPO_4, 1 *M* NaCl pH 7 followed by 50 m*M* NaH_2PO_4, 1 *M* NaCl pH 6.0. Purified nanobody was obtained after elution with 10 ml 50 m*M* sodium acetate pH 4.7 and was immediately neutralized by collecting it in tubes containing 2 ml 1 *M* Tris–HCl pH 7.5. The nanobody was further purified by gel filtration on a Superdex 75 HR 10/30 column equilibrated in 20 m*M* Tris–HCl pH 7.5, 150 m*M* NaCl; fractions containing 99% pure nanobody were pooled and concentrated using an ultrafiltration unit (3000 molecular-weight cutoff, Millipore). The protein concentration was estimated from the A_{280} as determined using a NanoDrop spectrophotometer (Thermo Scientific) using a value of 21 555.0 M^{-1} cm^{-1} for the extinction coefficient and the protein was stored at 277 K; 1 l of culture yielded 10 mg of pure protein (Fig. 1).

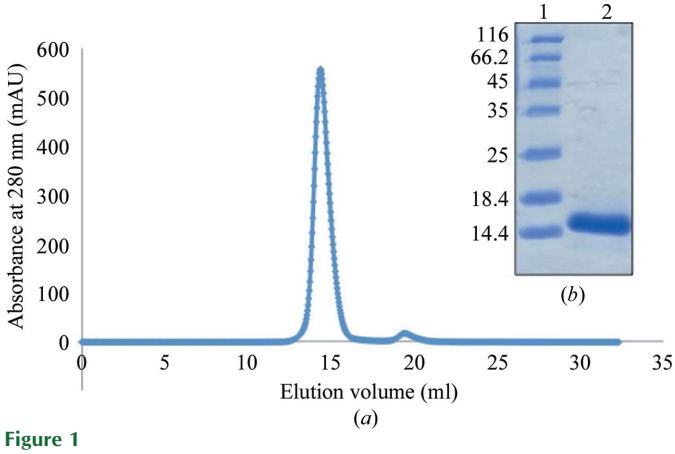

Figure 1
(*a*) Size-exclusion chromatography peak of Nb_PrP_01 on Superdex 75 HR 10/300; the running buffer was 20 m*M* Tris–HCl pH 7.5, 150 m*M* NaCl. (*b*) SDS–PAGE of purified Nb_PrP_01 (15% polyacrylamide gel stained with Instant Blue). Lane 1, molecular-weight markers (labelled in kDa); lane 2, Nb_PrP_01 (1 µl).

2.2. Protein crystallization

An extensive screening of crystallization conditions was performed using eight commercial screens from Hampton Research and Jena Bioscience (Index, Crystal Screen, Crystal Screen 2, PACT, JCSG, JBScreen Classic 1–4 HTS, JBScreen Classic 5–8 HTS and JBScreen Basic HTS) and three different protein concentrations (10, 30 and 71 mg ml^{-1}) in 96-well Intelli-Plates (Art Robbins Instruments) set up using a Phoenix crystallization robot (Art Robbins Instruments).

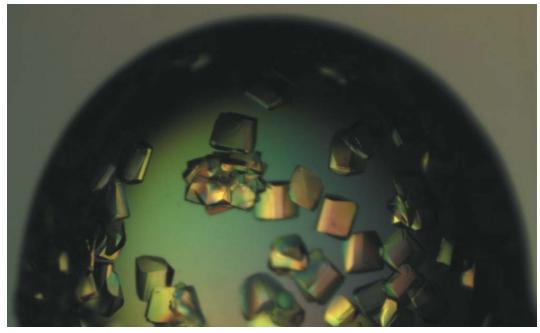

Figure 2
Crystals of Nb_PrP_01 grown in a seeded hanging drop in a 24-well Hampton Research plate.

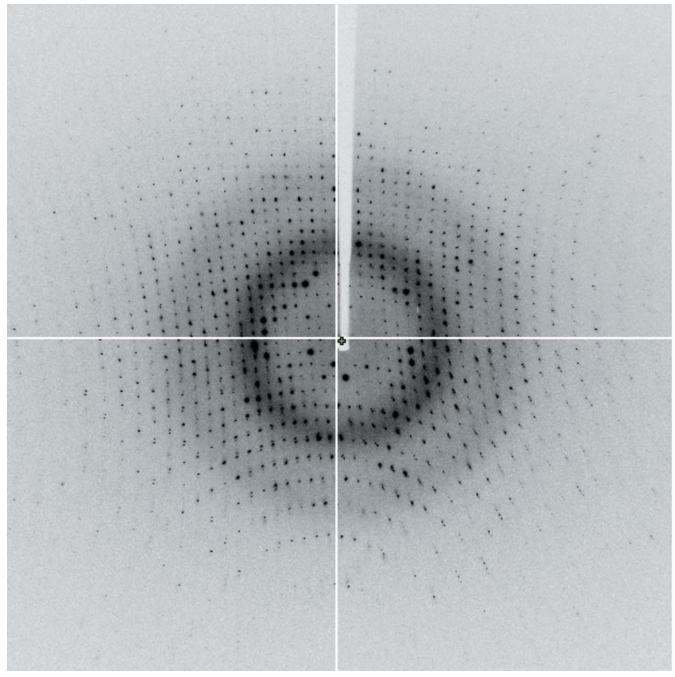

Figure 3
A representative 1° oscillation image of data collected from a crystal of Nb_PrP_01 using synchrotron radiation. The image was collected from a crystal cryocooled at 100 K using an ADSC Q4 detector on the ID14-2 beamline at ESRF, Grenoble, France.

Table 1
Data-collection and structure-solution statistics.

Values in parentheses are for the outer shell.

Crystal data	
Crystal dimensions (mm)	0.16 × 0.12 × 0.12
Matthews coefficient V_M (Å^3 Da^{-1})	1.5
Solvent content (%)	25.68
Unit-cell data	
Crystal system	Orthorhombic
Space group	$P2_12_12_1$
Unit-cell parameters (Å, °)	a = 30.4, b = 37.15, c = 83.00, $\alpha = \beta = \gamma = 90$
No. of molecules in unit cell Z	4
Wavelength (Å)	0.933
Temperature (K)	100
Resolution range (Å)	52.85–1.23 (1.29–1.23)
No. of unique reflections	27509
No. of observed reflections	189551
Completeness (%)	98.8 (98.3)
Multiplicity	3.0 (2.9)
$\langle I/\sigma(I)\rangle$	11.8 (4.4)
R_{merge} (%)	5.4 (19.4)

The sitting-drop vapour-diffusion method was used, with 100 nl protein sample mixed with an equal volume of screening solution. Although eight different screens were used, only condition C10 from JB Screen Basic HTS (catalogue No. CS-203; 30% PEG 4000, 0.2 *M* $MgCl_2$, 0.1 *M* Tris pH 8.5) produced one crystal at 293 K (Fig. 2) at the highest protein concentration (71 mg ml^{-1}). The crystal appeared in 3 d and reached maximum dimensions of 0.16 × 0.12 × 0.12 mm in 6 d. The crystal was reproduced in 24 h by streak-seeding (with a cat whisker) from the original drop into six hanging drops (in a 24-well plate from Hampton Research), in which the PEG 4000 concentration was varied from 24 to 34% with a 2% increment. Crystals from seeding were smaller in size (0.1 × 0.05 × 0.05 mm). A data set was collected from a crystal grown in 28% PEG 4000, 0.2 *M* $MgCl_2$, 0.1 *M* Tris pH 8.5.

3. Results and discussion

A complete X-ray diffraction data set was collected from a single crystal of nanobody Nb_PrP_01 which was cryocooled in liquid nitrogen using the reservoir solution containing 15% glycerol as a cryoprotectant. The X-ray diffraction data were collected on an ADSC Q4 CCD detector using synchrotron radiation on beamline ID14-2 (ESRF, Grenoble, France). The data-collection strategy was as follows: 100 images were collected with an oscillation step of 1° and 1 s exposure time. The crystal-to-detector distance was 96.4 mm.

The data set extended to 1.23 Å resolution (Fig. 3). Indexing was performed using *iMOSFLM* (Leslie, 1992) and scaling and merging were performed using the *CCP*4 package (Collaborative Computational Project, Number 4, 1994).

The crystal was found to belong to the orthorhombic space group $P2_12_12_1$, with unit-cell parameters a = 30.04, b = 37.15, c = 83.00 Å; the statistics are shown in Table 1. A total of 27 509 unique reflections were measured, with an average multiplicity of 3.0. The merged data set was 98% complete to 1.23 Å resolution, with an R_{merge} of 5.4% and a mean $I/\sigma(I)$ of 11.8 for all reflections and of 4.4 for the highest resolution shell. The calculated Matthews coefficient (V_M) of 1.5 Å^3 Da^{-1} indicates the presence of one Nb_PrP_01 molecule in the asymmetric unit, with a solvent content of 25.68% (Matthews, 1968; Collaborative Computational Project, Number 4, 1994). Although the solvent content is rather low, this is not uncommon for crystals that diffract to high resolution; previous cases have been reported with even lower solvent contents for exceptionally well diffracting crystals (Madhusudan *et al.*, 1993; Mandal *et al.*, 2009). The low solvent content may explain why this crystal diffracts to such high resolution.

The crystal structure of Nb_PrP_01 together with the already known mouse PrP^C structure (Riek *et al.*, 1996) may shed light on the nature of the PrP^C/PrP^{Sc} transition mechanism. Docking of the structures could provide useful information as to how the interaction between Nb_PrP_01 and mouse PrP^C can inhibit the pathogenic transition.

References

Antonyuk, S. V., Trevitt, C. R., Strange, R. W., Jackson, G. S., Sangar, D., Batchelor, M., Cooper, S., Fraser, C., Jones, S., Georgiou, T., Khalili-Shirazi, A., Clarke, A. R., Hasnain, S. S. & Collinge, J. (2009). *Proc. Natl Acad. Sci. USA*, **106**, 2554–2558.

Birkmann, E. & Riesner, D. (2008). *Prion*, **2**, 67–72.

Collaborative Computational Project, Number 4 (1994). *Acta Cryst.* D**50**, 760–763.

Conrath, K., Lauwereys, M., Galleni, M., Matagne, A., Frère, J., Kinne, J., Wyns, L. & Muyldermans, S. (2001). *Antimicrob. Agents Chemother.* **45**, 2807–2812.

Korotkov, K., Pardon, E., Steyaert, J. & Hol, W. (2009). *Structure*, **17**, 255–265.

Lam, A. Y., Pardon, E., Korotkov, K. V., Hol, W. G. & Steyaert, J. (2009). *J. Struct. Biol.* **166**, 8–15.

Lauwereys, M., Arbabi Ghahroudi, M., Desmyter, A., Kinne, J., De Holzer, W., Genst, E., Wyns, L. & Muyldermans, S. (1998). *EMBO J.* **17**, 3512–3520.

Leslie, A. G. W. (1992). *Jnt CCP4/ESF–EACBM Newsl. Protein Crystallogr.* **26**.

Madhusudan, Kodandapani, R. & Vijayan, M. (1993). *Acta Cryst.* D**49**, 234–245.

Mandal, K., Pentelute, B. L., Tereshko, V., Thammavongsa, V., Schneewind, O., Kossiakoff, A. A. & Kent, S. B. H. (2009). *Protein Sci.* **18**, 1146–1154.

Matthews, B. W. (1968). *J. Mol. Biol.* **33**, 491–497.

McKintosh, E., Tabrizi, S. J. & Collinge, J. (2003). *J. Neurovirol.* **9**, 183–193.

Riek, R., Hornemann, S., Wider, G., Billeter, M., Glockshuber, R. & Wüthrich, K. (1996). *Nature (London)*, **382**, 180–182.

Saerens, D., Frederix, F., Reekmans, G., Conrath, K., Jans, K., Brys, L., Huang, L., Bosmans, E., Maes, G., Borghs, G. & Muyldermans, S. (2005). *Anal. Chem.* **77**, 7547–7555.

Smolarek, D., Hattab, C., Hassanzadeh-Ghassabeh, D., Cochet, S., Gutiérrez, C., De Brevern, A., Udomsangpetch, R., Picot, J., Grodecka, M., Wasniowska, K., Muyldermans, S., Colin, Y., Le Van Kim, C., Czerwinski, M. & Bertrand, O. (2010). *Cell. Mol. Life Sci.* **67**, 3371–3387.

Van den Abbeele, A., De Clercq, S., De Ganck, A., De Corte, V., Van Loo, B., Soror, S. H., Srinivasan, V., Steyaert, J., Vandekerckhove, J. & Gettemans, J. (2010). *Cell. Mol. Life Sci.* **67**, 1519–1535.

Watts, J. C., Huo, H., Bai, Y., Ehsani, S., Jeon, A. H., Shi, T., Daude, N., Lau, A., Young, R., Xu, L., Carlson, G. A., Williams, D., Westaway, D. & Schmitt-Ulms, G. (2009). *PLoS ONE*, **28**, e7208.